Structure and rare-earth magnetism in $(Nd_{1-x}Gd_x)_2CuO_4$

P. Adelmann, R. Ahrens, G. Czjzek, G. Roth, H. Schmidt, and C. Steinleitner
Kernforschungszentrum Karlsruhe, P.O. Box 3640, W-7500 Karlsruhe 1, Federal Republic of Germany
(Received 15 January 1992; revised manuscript received 26 March 1992)

Mixed compounds $(Nd_{1-x}Gd_x)_2CuO_4$ with T' structure have been studied by x-ray diffraction, by measurements of the specific heat and of the magnetic susceptibility, and by ^{155}Gd Mössbauer spectroscopy. For Gd contents larger than a critical concentration $x_{cr}^s=0.625$, marked by a discontinuity in the concentration dependence of the lattice parameters a and c, the sites of O(1) atoms in the CuO_2 planes deviate from the symmetrical position in the T' structure. The deviations correspond to rotations of the O(1) squares around the central Cu sites. These distortions lower the local symmetry at Gd sites, which is orthorhombic for $x>x_{cr}^s$. However, x-ray-diffraction patterns show the global symmetry to be tetragonal for all compounds. The distortions provide an explanation for the magnetic properties of Gd-rich compounds, in particular for their weak ferromagnetism. A second critical concentration, $x_{cr}^m\sim0.4$, appears in the concentration dependence of the ordering temperature T_N^R of rare-earth moments. For $x>x_{cr}^m$, T_N^R increases linearly with x, from $T_N^R=1.95$ K for $x=0.46$ to $T_N^R=6.5$ K for $x=1$. For all $x<x_{cr}^m$, a Schottky maximum of the specific heat near 1.6 K indicates induced ordering of the rare-earth moments due to interactions with the ordered Cu moments.

I. INTRODUCTION

Rare-earth cuprates of composition R_2CuO_4 (R =Pr,Nd,Sm,Eu) with the tetragonal T' structure (Fig. 1) play a unique role among cuprates, becoming superconductors when suitably doped. For all other cuprates known so far, superconductivity is obtained when the number of electrons in the valence band is reduced, for example, when trivalent rare-earth ions are partly replaced by divalent Ba or Sr. In contrast, T'-structure compounds become superconductors when some rare-earth ions are replaced by cerium (for R =Pr,Nd,Sm,Eu) or by thorium (for R =Pr,Nd,Sm).[1] The charge state of thorium ions in these compounds is 4+ and the average charge state of cerium was determined to be close to 3.5+, near that in CeO_2.[2] Thus, in these compounds, the current carriers are electrons rather than holes as in the other cuprates.[2] Gd_2CuO_4 is the only rare-earth cuprate with T' structure in which superconductivity cannot be induced, neither by doping with cerium nor with thorium. In mixed compounds $(Nd_{1-x}Gd_x)_{1.85}Ce_{0.15}CuO_4$, T_c was found to decrease rapidly with increasing Gd content, dropping to zero for $x\sim0.6$.[1]

Apart from the overwhelming interest in the doped superconductors, questions of structural stability and of magnetic properties of both doped and undoped compounds have attracted attention. The tetragonal T' structure, shown in Fig. 1, is a variant of the K_2NiF_4 structure, also known as T structure. The difference is the position of O(2) atoms, which are situated approximately in one plane with R atoms in the T structure, completing a distorted octahedral oxygen coordination for the Cu atoms. This is the high-temperature tetragonal structure of La_2CuO_4. Below about 450 K, the oxygen octahedra are tilted about the [110] direction,[3] hence the crystal symmetry is reduced to orthorhombic. This distortion indicates that La_2CuO_4 is close to the limit of stability of the T structure. Indeed, in solid solutions $(La_{1-x}R_x)_2CuO_4$, R =Pr,Nd, rather small concentrations of the smaller rare-earth atoms (for Pr, $x\sim0.2$; for Nd, $x\sim0.1$) suffice to induce an abrupt change to the T' structure.[4] The range of stability of the T' structure is not very large, extending only from Pr_2CuO_4 to Gd_2CuO_4. For heavier—and smaller—rare-earth atoms and for Y, only cuprates of composition $R_2Cu_2O_5$ are obtained under ambient pressure. Recently, however, successful high-pressure synthesis of T'-structure compounds R_2CuO_4 with R =Y, Dy, Ho, Er, and Tm has been reported.[5,6]

Magnetic ordering of the Cu moments has been found in all T'-type rare-earth cuprates,[7] with Néel temperatures T_N^{Cu} in the range $250\le T_N^{Cu}\le280$ K. Variations in the values of T_N^{Cu} reported for the same compound may be caused by variations of oxygen content, which are

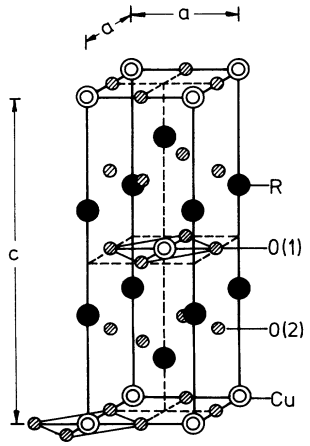

FIG. 1. T' structure of compounds R_2CuO_4 (R =Pr, Nd, Sm, Eu, Gd).

known to affect the ordering temperature of the Cu moments in La_2CuO_4 quite strongly.[3] Below T_N^{Cu}, weak ferromagnetism, ascribed to canting of Cu moments away from the collinear arrangement, has been observed in Gd_2CuO_4,[8] in several compounds containing mixtures of rare earths such as, for example, $SmGdCuO_4$, $EuTbCuO_4$, and $EuDyCuO_4$,[7] and in cuprates with Y and with heavy rare earths prepared under high pressure.[6] In the cuprates of Pr, Nd, and Sm, no indications for the presence of weak ferromagnetism have been found.[7]

As pointed out in Ref. 7, a prerequisite for the occurrence of weak ferromagnetism is a deviation from square-planar Cu-O coordination, either due to magnetoelastic stress or due to a structural distortion such that antisymmetric exchange interactions between Cu moments can be effective. Displacements of O(1) atoms from their ideal positions have been inferred from single-crystal x-ray-diffraction data for Gd_2CuO_4.[9] These displacements lower the symmetry of the Cu-O(1) planes in a way that is compatible with the existence of nonvanishing antisymmetric exchange interactions.[10]

Ordering of rare-earth moments has been inferred from specific-heat measurements for Sm_2CuO_4 and for Gd_2CuO_4, below the Néel temperatures $T_N^{Sm}=5.95$ K (Refs. 11 and 12) and $T_N^{Gd}=6.66$ K,[11] respectively. In both cases, the ordering temperature T_N^R is clearly marked by a sharp peak of the specific heat. In contrast, the low-temperature specific heat of Nd_2CuO_4 goes through a rounded maximum near 1.7 K.[11] This has been interpreted as indication for antiferromagnetic ordering of the Nd moments below $T_N^{Nd}=1.7$ K.[11] However, as shown in Ref. 13, the temperature dependence of the specific heat of Nd_2CuO_4 is qualitatively described as a Schottky anomaly associated with a temperature-independent splitting of the $4f$ ground-state doublet. For the splitting Δ, ascribed to Nd-Cu exchange interactions, the value $\Delta=0.76$ meV was assumed in Ref. 13. High-resolution inelastic neutron-scattering data obtained at 1.5 K have revealed a ground-state splitting $\Delta=0.35$ meV.[14]

Antiferromagnetic ordering of Nd moments at low temperatures has been confirmed by neutron diffraction.[15,16] The intensity of the relevant diffraction peaks, however, builds up gradually with decreasing temperature. There is no indication for an abrupt increase expected at a magnetic phase transition.

Thus, in spite of the overall similarity of T'-type rare-earth cuprates, there are subtle differences between compounds with different rare earths both in structural aspects and in magnetic properties. This has led us to investigate mixed compounds $(Nd_{1-x}Gd_x)_2CuO_4$, employing several complementary experimental techniques which are described in Sec. II. Results are presented in Sec. III, and their interpretation in terms of basic physical mechanisms is discussed in Sec. IV.

II. SAMPLES AND EXPERIMENTAL TECHNIQUES

A. Sample preparation

Starting materials were oxide powders Nd_2O_3, Gd_2O_3, and CuO of 99.999% purity. Appropriate amounts corresponding to the intended concentrations were thoroughly mixed in a ball mill and then subjected to the following heat treatments in air: (i) 20 h at 900 °C, (ii) 20 h at 900 °C, and (iii) 16 h at 1050 °C.

After (i), the reaction product was reground in a ball

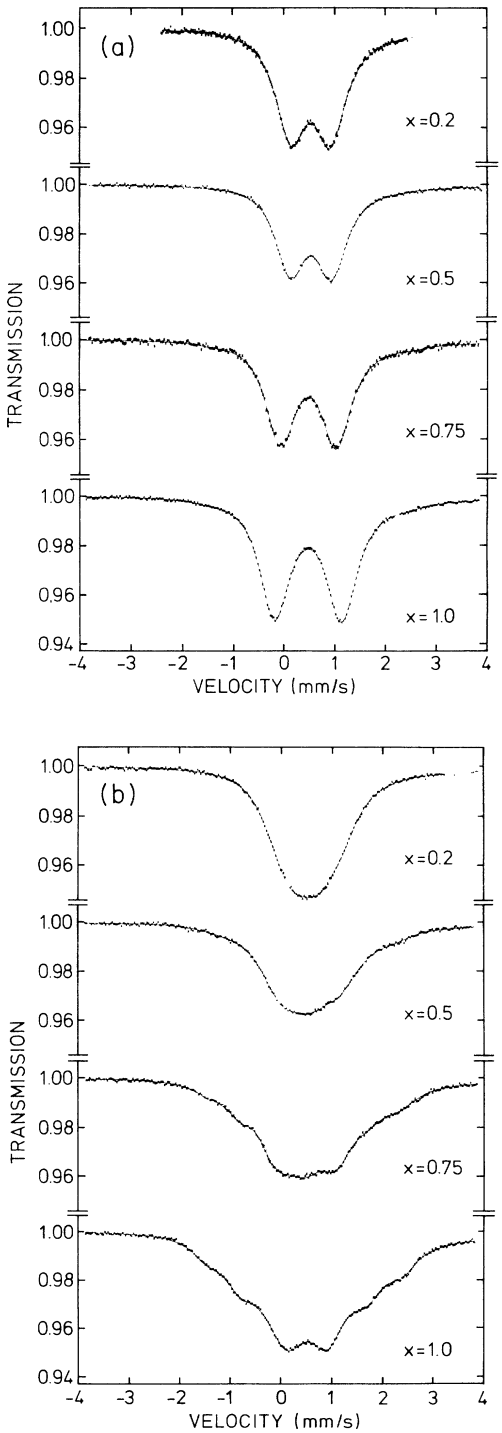

FIG. 2. ^{155}Gd Mössbauer spectra of several samples $(Nd_{1-x}Gd_x)_2CuO_4$ for the absorber temperatures (a) $T_A=30$ K, (b) $T_A=1.6$ K. Continuous lines show the results of least-squares fits.

mill, after (ii) the material was reground again and pressed to pellets. Alumina crucibles were employed for the heat treatments.

B. X-ray diffraction

Samples of the pure compounds Nd_2CuO_4 and Gd_2CuO_4 contained single-crystalline grains that were sufficiently large ($\sim 10^3$ μm^3) for single-crystal diffraction. For both compounds, four-circle diffractometer measurements were done at room temperature, for Gd_2CuO_4 also at 30 K, with Mo $K\alpha$ radiation ($\lambda = 0.7103$ Å) for scattering angles up to $2\theta = 90°$ ($\pm h, \pm k, \pm l$). The structure refinement was done by least-squares fits with the full matrix.

For the mixed compounds $(Nd_{1-x}Gd_x)_2CuO_4$, $0 < x < 1$, powder-diffraction patterns were obtained at room temperature using Cu K_α radiation ($\lambda = 1.54056$ Å) in the range of scattering angles $10° \leq 2\theta \leq 125°$. A position-sensitive detector with a resolution of 0.1° full width at half maximum (FWHM) was employed. The diffraction patterns were analyzed by Rietveld line profile refinement.

C. Calorimetry and magnetic measurements

The specific heat of compact pieces (about 60 mg) cut from the pellets was measured with a semiadiabatic heat-pulse calorimeter in the temperature range $1.5 \leq T \leq 45$ K. For Nd_2CuO_4 and Gd_2CuO_4, the specific heat was also measured in a magnetic field of 4.4 T.

A Faraday balance was employed for measurements of the magnetic susceptibility in the temperature range from 1.7 to 300 K. The applied field was 50 mT.

D. Mössbauer spectroscopy

Mössbauer spectra of ^{155}Gd were taken with a conventional constant-acceleration spectrometer. The source, ^{155}Eu:*Pd*, was immersed in liquid He. The linewidth of recoilless emitted radiation, $\Gamma_s = (0.35 \pm 0.01)$ mm s^{-1}, was slightly larger than the natural linewidth, $\Gamma_{nat} = 0.250 \pm 0.003$ mm s^{-1}.

Absorbers were made of powdered compounds with thickness in the range 2.0–2.7 kg m^{-2}. For Gd concentrations $x \geq 0.35$, natural Gd_2O_3 was used in the preparation. For $x = 0.2$, natural Gd_2O_3 and oxide with ^{155}Gd enriched to 90.5% were mixed in the ratio 3:1. For all compounds studied, spectra were taken for absorber temperatures $T_A = 30$ K [Fig. 2(a)], $T_A = 4.2$ and 1.6 K [Fig. 2(b)].

The spectra were analyzed by nonlinear least-squares fits of the transmission integral with numerical diagonalization of the hyperfine Hamiltonian.

III. RESULTS

A. Structural aspects

The reflections observed in the x-ray-diffraction patterns of all samples could be indexed in the space group $I4/mmm$ corresponding to the T' structure displayed in Fig. 1. However, the single-crystal data for Gd_2CuO_4 yielded an anomalous elongation of the ellipsoids for O(1) occupation probabilities, with the long axis pointing in a direction perpendicular to the c axis and perpendicular to the Cu-O(1) bonds, as illustrated in Fig. 3. Since the elongations have the same value at 30 K and at room temperature, thermal vibrations can be excluded as cause; rather, these elongations must be ascribed to static displacements of O(1) atoms by ±0.18 Å from the symmetric positions in the direction of the long axes of the ellipsoids. There is no indication for an anomalous out-of-plane component of the displacements. These results are in agreement with those reported in Ref. 9.

Additional information about the structure was derived from low-temperature ($T = 1.6$ K) ^{155}Gd Mössbauer spectra. Large values of the asymmetry parameter $\eta = (V_{xx} - V_{yy})/V_{zz}$ show the local symmetry at Gd sites to be orthorhombic. In addition, the absence of any broadening of the resonance absorption lines implies the absence of significant variations of the local structure from site to site. This suggests ordered O(1) displacements as indicated by hatched circles in Fig. 3.

Since neither superstructure reflections nor splittings of reflections corresponding to the tetragonal T' structure could be detected in the single-crystal diffractograms, three-dimensional long-range order of the displacements in our crystals appears rather unlikely. However, superstructure reflections indicating ordered displacements have been observed in an electron-diffraction study of Gd_2CuO_4 single crystals.[17]

The lattice parameters a and c of mixed compounds vary linearly with Gd concentration x for $0 \leq x \leq 0.625$, and again for $0.625 \leq x \leq 1$ (Fig. 4). At the critical concentration $x_{cr}^s = 0.625$, the slopes and also the values of a and c change abruptly. This discontinuity is reflected in the concentration dependence of the unit-cell volume [Fig. 5(a)] and of the axial ratio $c/3a$ [Fig. 5(b)], as well.

The structural change at x_{cr}^s leads to a drastic change of the electric-field-gradient tensor at ^{155}Gd nuclei (Fig. 6). This change cannot be seen in the quadrupole splitting of Mössbauer spectra obtained at the absorber temperature $T_A = 30$ K [Fig. 2(a)]. Only the ground state of ^{155}Gd nuclei with spin $I_g = \frac{3}{2}$ has a sizeable quadrupole

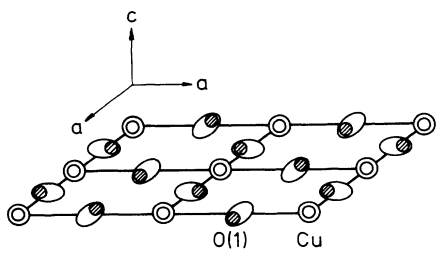

FIG. 3. Distorted Cu-O(1) plane in Gd_2CuO_4. Ellipses mark the elongated O(1)-occupation regions inferred from single-crystal x-ray diffraction. The orthorhombic symmetry at Gd sites, located above and below the centers of the squares bounded by Cu atoms, implies short-range ordered displacements of O(1) atoms to the positions marked by hatched circles.

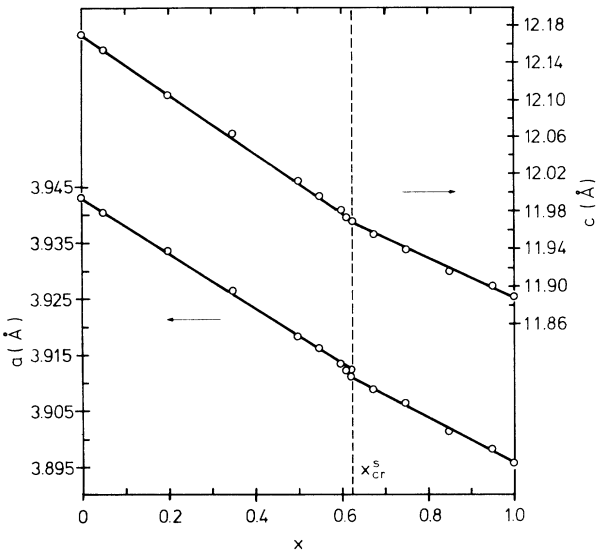

FIG. 4. Dependence of the lattice parameters a and c upon Gd concentration x in mixed compounds $(Nd_{1-x}Gd_x)_2CuO_4$. When no error bars are indicated, standard error estimates did not exceed the size of the symbols used to mark the results. Straight lines show results of linear least-squares fits.

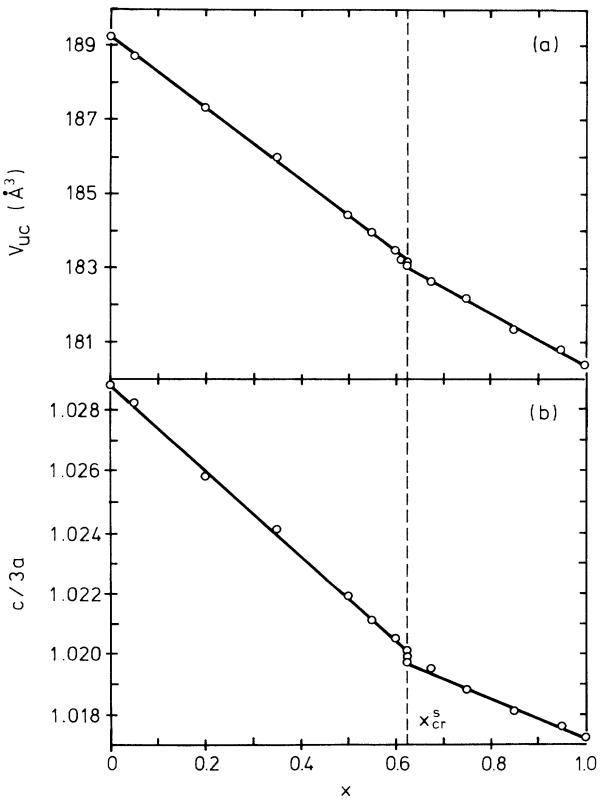

FIG. 5. Variation (a) of the unit-cell volume V_{uc} and (b) of the axial ratio $c/3a$ with Gd concentration x in $(Nd_{1-x}Gd_x)_2CuO_4$. Straight lines show results of linear least-squares fits.

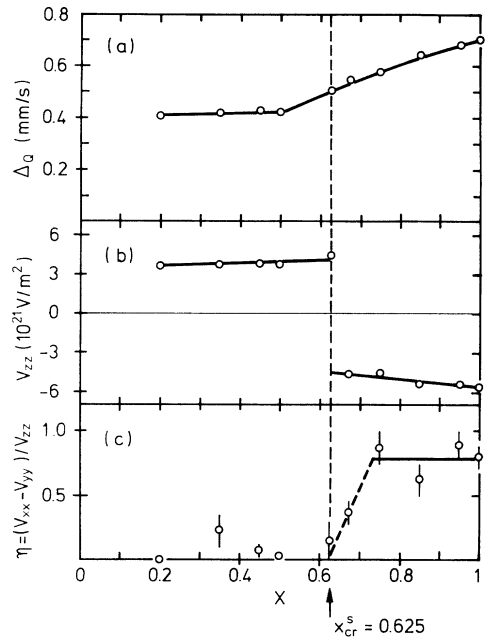

FIG. 6. Dependence (a) of the quadrupole splitting Δ_Q, defined in Eq. (1), (b) of V_{zz}, the z component of the electric-field-gradient tensor, and (c) of the asymmetry parameter η upon Gd concentration x in $(Nd_{1-x}Gd_x)_2CuO_4$. Lines serve as guides to the eye.

moment, $Q_g = 1.30 \pm 0.02$ b,[18] leading to an observable splitting into two levels separated by

$$2\Delta_Q = \tfrac{1}{2} e Q_g |V_{zz}| (1+\eta^2/3)^{1/2} . \quad (1)$$

The splitting of the excited nuclear state with spin $I_e = \frac{5}{2}$, $Q_e = 0.12 \pm 0.02$ b,[19] is small compared to the linewidth. Thus, it is not resolved. Figure 6(a) shows the smooth decrease of the ground-state splitting Δ_Q with decreasing Gd content x through the critical concentration x^s_{cr} until $x = 0.5$. At this latter concentration, the slope $d\Delta_Q/dx$ drops to a very small value, and Δ_Q hardly changes between $x = 0.2$ and $x = 0.5$.

Spectra obtained at $T_A = 1.6$ K [Fig. 2(b)] with antiferromagnetic order of the rare-earth moments, in contrast, are sensitive to the value of η and to the sign of V_{zz} as well as to the direction of the magnetic hyperfine field with respect to the principal axes of the field-gradient tensor. The concentration dependences of V_{zz} and η, displayed in Figs. 6(b) and 6(c), respectively, clearly show two effects occurring in coincidence with the structural change at the critical concentration: (i) the sign of V_{zz} changes from $V_{zz} > 0$ for $x \leq x^s_{cr}$ to $V_{zz} < 0$ for $x > x^s_{cr}$, and (ii) the asymmetry parameter η has large nonzero values for $x > x^s_{cr}$, whereas for $x < x^s_{cr}$, the values of η are small, compatible with $\eta = 0$ as expected for tetragonal symmetry.

Thus, displacements of O(1) atoms from symmetrical positions (Fig. 3) appear abruptly at the critical concentration x^s_{cr}.

As the results for V_{zz} and η are derived from spectra obtained in the presence of ordered rare-earth moments,

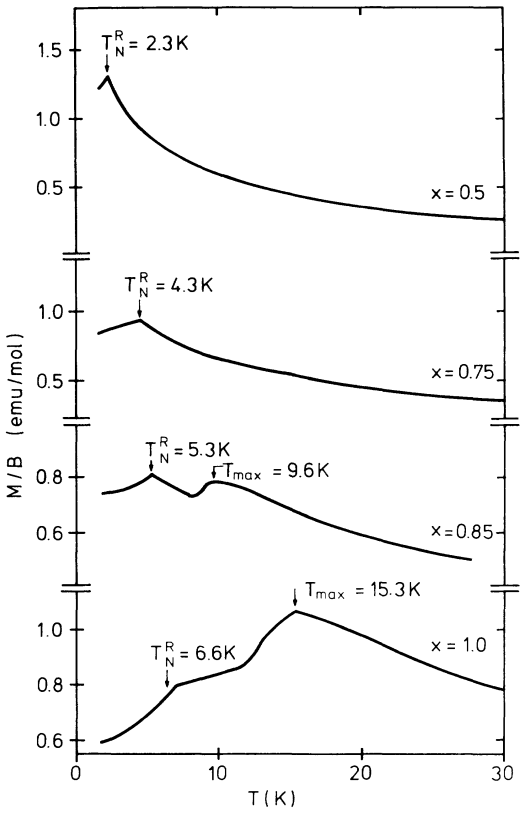

FIG. 7. Temperature dependence of the molar magnetic susceptibility of some Gd-rich compounds $(Nd_{1-x}Gd_x)_2CuO_4$ below 30 K, measured in an applied field $B = 50$ mT.

distortions induced by the ordering of rare-earth moments at T_N^R cannot be excluded *a priori*. However, the splitting Δ_Q, calculated with these values according to Eq. (1), agrees perfectly with the splitting observed at 30 K, well above T_N^R, for all samples. This finding renders a magnetoelastic distortion at T_N^R highly unlikely. Furthermore, the x-ray-diffraction data for the Gd_2CuO_4 single crystal show the distortions to remain essentially unchanged up to room temperature, above T_N^{Cu}. However, a transition to tetragonal symmetry may occur at some higher temperature.

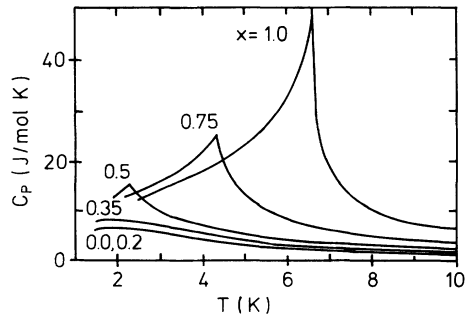

FIG. 8. Low-temperature specific heat of several compounds $(Nd_{1-x}Gd_x)_2CuO_4$.

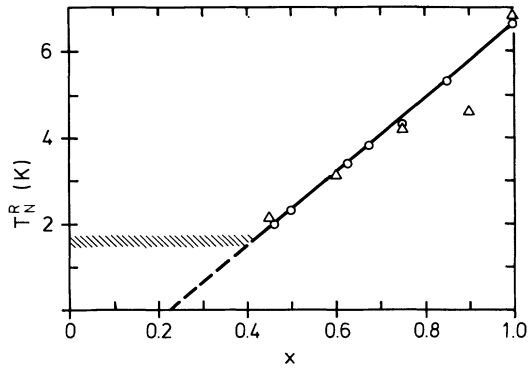

FIG. 9. Concentration dependence of the ordering temperatures T_N^R of rare-earth moments. Circles: our results, deduced from specific-heat measurements. Triangles: results reported in Ref. 20. The hatched region for Gd concentrations $x \leq 0.4$ marks the position of the maximum in the specific heat, which we interpret as a Schottky anomaly rather than as an indication for spontaneous ordering of rare-earth moments.

Information about local changes of the electronic structure can be deduced from the center shift of the resonance absorption spectrum, the isomer shift, which is linearly related to the electron density at the position of the ^{155}Gd nuclei. In compounds $(Nd_{1-x}Gd_x)_2CuO_4$, the isomer shift changes gradually with Gd content x by a

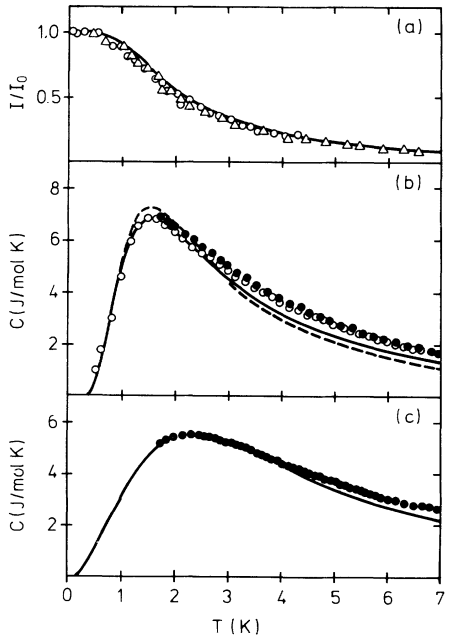

FIG. 10. Experimental evidence supporting the interpretation of the specific-heat anomaly in Nd_2CuO_4 as a Schottky anomaly. (a) Variation of the intensity of neutron reflections due to magnetic order of Nd moments. Circles: from Ref. 15; triangles: from Ref. 16. (b) Low-temperature specific heat of Nd_2CuO_4, measured in zero field. Open circles: results of Ref. 11; full circles; results of the present work. (c) Specific heat of Nd_2CuO_4, measured in an applied field of 4.4 T. The lines show the results of our calculations described in Sec. IV C.

small amount, from $\delta_{IS}=0.517\pm0.001$ mm/s for $x=0.2$ to $\delta_{IS}=0.500\pm0.001$ mm/s for $x=1$.

B. Rare-earth magnetism

The temperature dependence of the magnetization measured in a constant field of 50 mT in the temperature region from 1.8 to ~35 K is shown in Fig. 7 for several samples. The maximum appearing above T_N^{Gd} in Gd-rich samples is caused by the weak ferromagnetism as shown in detail in Refs. 7 and 8 for Gd_2CuO_4. When Nd is introduced, the maximum shifts to lower temperatures, and it weakens rapidly. For $x\leq0.75$, no maximum of the susceptibility is discernible at any temperature above T_N^R. Our data for the mixed compounds are quite similar to those reported in Ref. 20.

The effect of weak ferromagnetism upon the temperature dependence of the magnetization prohibits a precise determination of the ordering temperature T_N^R of the rare-earth moments in Gd-rich compounds. Thus, we have measured the specific heat of the samples at low temperatures (Fig. 8). For samples with Gd content $x\geq0.45$, T_N^R is clearly marked by a sharp peak of the specific heat. As shown in Fig. 9, $T_N^R(x)$ varies linearly with x in this concentration range. For smaller Gd concentrations, $x\leq0.35$, no peak was found in the temperature range accessible in our calorimeter ($T\geq1.5$ K). Instead, a rounded maximum, similar to that reported in Ref. 11, appeared at about 1.6 K for samples in this range of concentrations. These results indicate a second critical concentration $x_{cr}^m\sim0.4$ separating regions that differ in the low-temperature behavior of the rare-earth moments.

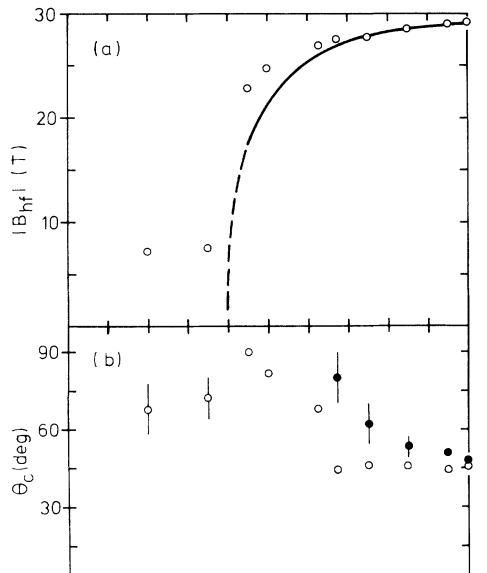

FIG. 11. Concentration dependence (a) of the absolute value of the hyperfine fields measured at 1.6 K, and (b) of the angle θ_c between the crystallographic c axis and the direction of the hyperfine field. The line in (a) shows the concentration dependence expected by molecular-field theory due to the change of T_N^R with Gd concentration, assuming a constant saturation value $|B_{hf}(T=0)|=29.6$ T. Open (closed) circles in (b) mark values of θ_c deduced under the assumption that the z axis of the EFG tensor is parallel (perpendicular) to the crystallographic c axis. For details, see the Appendix.

The specific heat of Gd_2CuO_4 in a field of 4.4 T is similar to that in zero field shown in Fig. 8. The peak is shifted to a slightly lower temperature, $T_N^{Gd}(B=4.4\text{ T})=6.3\pm0.1$ K, as expected for the phase transition to a state with antiferromagnetic order.

In contrast, in a field of 4.4 T, the maximum of the specific heat of Nd_2CuO_4 is shifted to a higher temperature. Furthermore, it is considerably broadened [Fig. 10(c)] compared to the zero-field data [Fig. 10(b)].

The concentration dependence of the magnetic hyperfine field B_{hf} at Gd nuclei, derived from Mössbauer spectra at 1.6 K, shows trends which appear related to the variation of $T_N^R(x)$ described [Fig. 11(a)]. Initially, $|B_{hf}|$ decreases slowly with decreasing x from its maximum value for Gd_2CuO_4. Below $x=0.46$, $|B_{hf}|$ drops precipitously and maintains a small, constant value in the Nd-rich compounds.

IV. DISCUSSION

A. Structural aspects, weak ferromagnetism in Gd_2CuO_4

The results described in Sec. III A reveal some similarity between the T'-structure compound Gd_2CuO_4 and La_2CuO_4 with T structure. In both cases, the structure is stabilized by a distortion involving oxygen atoms in the first coordination sphere of copper. However, different coordination geometries (squares and octahedra, respectively) lead to different characters of the distortions (rotation and tilting, respectively).

An incipient instability with rotational character is already indicated in the phonon dispersion curves of Nd_2CuO_4, determined by inelastic neutron scattering.[21] For the corresponding vibrational branch, a tendency to softening with the approach toward the boundary of the Brillouin zone ($\mathbf{Q}\rightarrow[\pi/a,\pi/a,0]$) has been found. In Nd_2CuO_4, the frequency of this mode at the zone boundary is lower by about 20% than in Pr_2CuO_4. In addition, an anomalous lowering of this frequency with decreasing temperature was found in Nd_2CuO_4.[21]

Obviously, the tendency to instability is related to the decreasing ionic radius of the rare earths. As smaller Gd atoms are substituted for Nd atoms in $(Nd_{1-x}Gd_x)_2CuO_4$, this trend is further nourished. At the critical Gd concentration $x_{cr}^s=0.625$, the limit of stability is reached, and for higher Gd concentrations the T' structure is maintained only in its distorted form.

The vibrational instability at the zone boundary is not observable by Raman spectroscopy, which is restricted to vibrational modes with $\mathbf{Q}=0$. However, in Raman spectra of Gd_2CuO_4, modes appear that are not compatible with the tetragonal T' structure.[22] The lowering of symmetry associated with rotations of the oxygen squares around copper should provide a basis for an assignment of these extra modes.

In addition, it is possibly of interest that in Ce-doped

compounds $(Nd_{1-x}Gd_x)_{1.85}Ce_{0.15}CuO_4$, the transition temperature to superconductivity approaches zero[1] for a Gd concentration that appears to be very close to the critical concentration $x_{cr}^{s}=0.625$ determined in the present work.

The lowering of symmetry associated with displacements of O(1) atoms from the symmetrical positions allows an antisymmetric Dzyaloshinsky[23]-Moriya[10] (DM) exchange term between adjacent copper moments,

$$H_{ij}^{DM}=\mathbf{D}\cdot[\mathbf{S}_i\times\mathbf{S}_j]\ , \tag{2}$$

to be effective. The direction of the Dzyaloshinsky vector **D** is determined by the point symmetry at the point bisecting the straight line between the Cu atoms coupled by the interaction, Eq. (2). According to the criteria given by Moriya,[10] for the distorted Cu-O(1) planes (Fig. 3), the direction of **D** is parallel to the crystallographic c axis. Thus, by Eq. (2), the antisymmetric exchange term involves only components of the Cu moments in the Cu-O(1) plane. This is in agreement with the conclusion that the weak ferromagnetic moment, and thus the canting of Cu moments, is parallel to the Cu-O(1) planes, derived from studies of Gd_2CuO_4 single crystals in Ref. 8.

Again, there is some similarity with La_2CuO_4. In this compound, canting of the Cu moments, ascribed to antisymmetric exchange interactions, has been observed as well.[24] However, the different geometry of the distortions leads to differences in details. In La_2CuO_4, the moments are canted out of the Cu-O(1) planes, and the weak ferromagnetism remains hidden when no field is applied since the moments cant in opposite directions in adjacent planes. Weak ferromagnetism is induced by application of a magnetic field parallel to the c axis, which is stronger than a temperature-dependent threshold value.

B. Rare-earth magnetism in Gd-rich compounds

For Gd-rich compounds, our results for the temperature T_N^R of the phase transition to antiferromagnetic order of rare-earth moments, deduced from specific-heat measurements (Fig. 8) agree with the values reported for Gd_2CuO_4,[11] and with most data of Ref. 20 for compounds $(Nd_{1-x}Gd_x)_2CuO_4$ $(x\geq 0.45)$. The slope $dT_N^R(x)/dx$ is surprisingly steep. Even for low Nd concentrations, it exceeds the slope expected in case of simple dilution with nonmagnetic atoms as it extrapolates to $T_N^R=0$ for $x=0.23$ rather than for $x=0$. This behavior indicates either the presence of competing interactions or some kind of incompatibility of Gd-Gd and Gd-Nd interactions. This may be related to different preferred directions of Gd and Nd moments deduced from low-temperature Mössbauer spectra.

As we discuss in the Appendix, a unique value for the angle θ between the crystallographic c axis and the direction of the hyperfine field, which coincides with the direction of the local Gd moment, cannot be derived from spectra of Gd-rich compounds with orthorhombic local symmetry. Two values of θ are possible in each case. However, for Gd_2CuO_4, we obtain $\theta=45°\pm 3°$ for both possibilities [Fig. 11(b)]. We interpret this result as an indication for noncollinear ordering of Gd moments in Gd_2CuO_4.

In Nd-rich compounds, in contrast, rare-earth moments point in a direction perpendicular to the c axis or at least nearly so, in agreement with results derived from neutron-diffraction studies of Nd_2CuO_4.[15,16] There, Nd moments were found to point in a [110] direction, perpendicular to the c axis. Fits to the Mössbauer spectra with the constraint $\theta=90°$ were satisfactory. For these compounds with tetragonal symmetry at the rare-earth site, the value of θ is unambiguous. Yet, the estimated errors of the results are quite large due to the small value of the hyperfine field.

In considering the variation of the hyperfine field $|B_{hf}|$, measured at 1.6 K, with Gd concentration x [Fig. 11(a)], we must first of all account for the variation of T_N^R, that is, of the ratio $1.6/T_N^R$, with x. We have calculated $|B_{hf}(x,T=1.6\ \text{K})|$ in the framework of molecular-field theory assuming the saturation field $|B_{hf}(x,T=0)|=29.6$ T not to depend upon x. The results, drawn as continuous line in Fig. 11(a), describe all experimental data for $x>0.6$. For smaller Gd concentrations, the experimental hyperfine fields progressively deviate toward larger values. Several reasons for these deviations are conceivable. A significant contribution to the deviations could stem from an increasing importance of exchange interactions between copper and rare-earth moments which seem to play a dominant role in Nd-rich compounds, to be discussed in Sec. IV C.

C. Rare-earth magnetism in Nd-rich compounds

The good agreement between our specific-heat values for Nd_2CuO_4, determined in the temperature range $1.7\leq T\leq 7$ K, and the data reported in Ref. 11 [Fig. 10(b)] for independently prepared samples, is strong evidence for the intrinsic nature of the specific-heat anomaly. It resembles a Schottky anomaly due to a temperature-independent level splitting of about 4 K [dashed line in Fig. 10(b)]. It must be emphasized that both our data and those of Ref. 11 refer to one mole of the formula unit containing two Nd atoms. Thus, the maximum value of the specific heat, $C_{exp}^{max}=6.81$ J/(mol K) is slightly less than expected for a Schottky anomaly [7.3 J/(mol K)], not larger as stated in Ref. 13. Furthermore, the entropy increase associated with the anomaly is close to $k_B\ln 2$ per Nd atom.

In principle, the anomaly could be caused by temperature-induced population of a low-lying excited crystal-field doublet, assuming that the crystal-field ground state is a doublet as well. However, the gradual buildup of static Nd moments in the temperature range of the anomaly, revealed by neutron diffraction [Fig. 10(a)],[15,16] proves the anomaly to be due to magnetic splitting of the ground-state doublet. The only conceivable cause for this splitting is an exchange interaction between copper and neodymium moments. As $T_N^{Cu}\geq 250$ K, the splitting is temperature independent in the temperature range of interest, $T\leq 10$ K.

The agreement with the experimental results is improved if we assume both Nd-Cu and Nd-Nd exchange

interactions to be effective. The latter are treated within a molecular-field approach:

$$\Delta(T)=\Delta_0+2B_{\mathrm{Nd}}\langle\mu_{\mathrm{Nd}}\rangle_T\ , \tag{3}$$

with

$$\langle\mu_{\mathrm{Nd}}\rangle_T=\mu_0\tanh[\Delta(T)/k_BT]\ . \tag{4}$$

$\Delta_0=2B_{\mathrm{Cu}}\mu_0$ is the temperature-independent splitting due to Cu-Nd interactions.

The solid line in Fig. 10(b) shows the calculated specific heat, obtained for self-consistent solutions of Eqs. (3) and (4), with the parameter values $\Delta_0=4.5$ K and $B_{\mathrm{Nd}}\mu_0=-0.4$ K.

The relative intensities of magnetic reflections, setting

$$I(T)/I_0=(\langle\mu_{\mathrm{Nd}}\rangle_T/\mu_0)^2\ , \tag{5}$$

calculated with the same parameter values, are given by the continuous line in Fig. 10(a). The experimental results of Refs. 15 and 16 are very well reproduced by this approach.

Discrepancies between experimental specific-heat data and calculations above ~ 2.5 K are mainly ascribed to shortcomings of the molecular-field approach. Lattice and electronic contributions, which should be comparable to the specific heat measured for the compounds with nonmagnetic rare earths, Pr_2CuO_4 and Eu_2CuO_4,[11] are too small to account for the differences.

Our interpretation of the specific-heat anomaly in Nd_2CuO_4 is further supported by the specific heat measured in an applied field of 4.4 T, displayed in Fig. 10(c). In this case, the results are well described if we assume a distribution $P(\Delta)$ of the splitting parameter Δ. A distribution of splittings is expected for a polycrystalline sample in an applied field $\mathbf{B}_a$ since the effective field $\mathbf{B}_{\mathrm{eff}}$ acting on the Nd moments is given by the vector sum

$$\mathbf{B}_{\mathrm{eff}}=\mathbf{B}_a+\mathbf{B}_{\mathrm{Cu}} \tag{6}$$

of the applied field and the exchange field $\mathbf{B}_{\mathrm{Cu}}$ due to copper moments. Thus, $\mathbf{B}_{\mathrm{eff}}$ varies with the orientation of the crystallites. For an isotropic distribution of the directions of $\mathbf{B}_{\mathrm{Cu}}$, the distribution of splittings $\Delta=2B_{\mathrm{eff}}\mu_0$ is easily shown to be given by

$$P(\Delta)=\begin{cases}\Delta/(2\Delta_0\Delta_a) & \text{for } |\Delta_a-\Delta_0|\le\Delta\le\Delta_a+\Delta_0\\ 0 & \text{for } \Delta<|\Delta_a-\Delta_0| \text{ and } \Delta>\Delta_a+\Delta_0\ ,\end{cases} \tag{7}$$

with $\Delta_a=2B_a\cdot\mu_0$, the splitting induced by the applied field $B_a=4.4$ T, and Δ_0 as defined before. The continuous curve in Fig. 10(c), calculated with parameter values $\Delta_a=5.0$, $\Delta_0=3.5$ and $B_{\mathrm{Nd}\cdot\mu_0}=-0.3$ K, closely follows the experimental data. The values for the parameters Δ_0 and $B_{\mathrm{Nd}\cdot\mu_0}$ are somewhat smaller than those derived from the analysis of the specific heat in zero field. A smaller value for Δ_0 can be expected if the orientations of the crystallites are not quite randomly distributed. From $\Delta_a=5.0$ K in a field of 4.4 T, we calculate $\mu_0=0.85\mu_B$, somewhat less than $\mu_0=1.3\mu_B$ derived from the intensity of magnetic neutron-diffraction peaks.[16]

The negative sign of the Nd-Nd exchange term $B_{\mathrm{Nd}\cdot\mu_0}$ shows that the Nd-Nd interaction is opposed to the ordering of Nd moments induced by the Cu moments. For the magnetic order in Nd_2CuO_4 deduced from neutron diffraction (Fig. 2 of Ref. 16), this implies either dominant ferromagnetic interactions between Nd neighbors in the *ab* plane (distance ~ 3.94 Å) or dominant antiferromagnetic interactions between Nd neighbors along the *c* axis (distance ~ 3.65 Å). In view of the general tendency to antiferromagnetic interactions between rare-earth moments in these cuprates, we believe the second alternative to be the correct one.

Qualitatively, the low-temperature specific heat does not change in compounds containing Gd up to the Gd concentration $x=0.35$ (Fig. 8). This is another indication for weak exchange interactions between Nd and Gd. Only for Gd concentrations $x\ge 0.46$, a clear signature of a phase transition to a state with antiferromagnetic order of rare-earth moments is observed. The change from Cu-induced ordering to spontaneous ordering of rare-earth moments, characterized by a Néel temperature T_N^R, seems to occur at the critical concentration $x_{\mathrm{cr}}^m\approx 0.4$. According to our results, displayed in Fig. 9, at this concentration, the value of $T_N^R(x_{\mathrm{cr}}^m)$ coincides with the temperature at which the Schottky specific heat has its maximum value.

The interpretation of the low-temperature specific heat of Nd_2CuO_4 in terms of a Schottky anomaly due to exchange interactions between Nd moments and static Cu moments provides a consistent explanation for all relevant experimental data (specific heat in zero field and in an applied magnetic field as well as magnetic neutron-diffraction intensities). In the light of this interpretation, the similarity of the specific-heat results[11] for the superconducting compounds $Nd_{1.85}Ce_{0.15}CuO_4$ and $Nd_{1.85}Th_{0.15}CuO_4$ to those for the undoped compound is rather surprising. In the doped compounds, static antiferromagnetic order of Cu moments can be ruled out.[15] Recently, however, an investigation of compounds $Nd_{2-y}Ce_yCuO_4$ by Raman spectroscopy has brought evidence for the preservation of *local* antiferromagnetic order of Cu moments up to high Ce concentrations ($y\le 0.2$).[25] If the fluctuation rate Γ_{Cu} of correlated Cu moments is not much larger than $\Delta_0/\hbar\sim 5\times 10^{11}$ s^{-1}, Nd-Cu exchange interactions may well induce a splitting of the Nd crystal-field ground state. Lifetime broadening and a reduced average splitting will lead to modifications of the specific-heat anomaly compared to undoped Nd_2CuO_4 as they have been observed experimentally.[11]

The low fluctuation rate invoked by this interpretation implies occurrence of elastic magnetic diffraction peaks if the correlations are three-dimensional. No diffraction peaks due to correlations of Cu moments have been found in powder-diffraction patterns of $Nd_{1.85}Ce_{0.15}CuO_4$.[15] In case of two-dimensional correlations, on the other hand, the elastic intensity is smeared out along linear streaks in the reciprocal lattice. This can be detected only by magnetic neutron diffraction on single crystals, which has not yet been reported for $Nd_{2-x}Ce_xCuO_4$. In $La_{2-x}Sr_xCuO_4$, however, slowly fluctuating two-dimensional correlations of Cu moments

have been observed at low temperatures for high levels of Sr doping ($x \leq 0.14$).[26]

Alternatively, the specific-heat anomaly in $Nd_{1.85}Ce_{0.15}CuO_4$ could be due to a Kondo effect as in diluted, metallic samples $Eu_{1-x}Pr_xBa_2Cu_3O_{7-\delta}$ ($x \leq 0.4$).[27] This interpretation, however, is not compatible with the observation of neutron-diffraction peaks due to magnetic ordering of Nd moments in $Nd_{1.85}Ce_{0.15}CuO_4$, reported in Ref. 15.

Additional information about the cause for the specific-heat anomaly may be obtained by specific-heat measurements in an applied field. As shown in Ref. 27, the maximum value of the specific heat increases in an applied field if the anomaly is caused by a Kondo effect. In contrast, we found the maximum value of the specific heat to decrease in an applied field in Nd_2CuO_4.

D. Charge density and crystal field at Gd sites

The isomer shifts near 0.5 mm/s are in the range that is typical for ionic Gd compounds,[28] close to the shifts in Gd_2O_3 and in $GdBa_2Cu_3O_{7-\delta}$.[29] The results indicate a rather low degree of covalent Gd-O bonding.

The variation of isomer shift with Gd concentration x seems to be entirely due to the reduction of electron density with increasing atomic volume as x decreases [Fig. 5(a)]. Converting results for ^{151}Eu and ^{153}Eu, derived from pressure experiments,[30] to the isomer shift scale for ^{155}Gd, the volume-dependent shift is estimated to be given by

$$\delta_{IS}(V)-\delta_{IS}(V_a)=a(V/V_a-1)\ , \tag{8}$$

with $0.3 \leq a \leq 0.6$ mm/s.

As shown in Fig. 12, the results for $(Nd_{1-x}Gd_x)_2CuO_4$ are described by Eq. (8) with $a=0.50\pm0.05$ mm/s, a value between the two limits given above. Thus, the isomer shift data indicate that the degree of Gd-O covalency remains low when Gd is replaced by Nd.

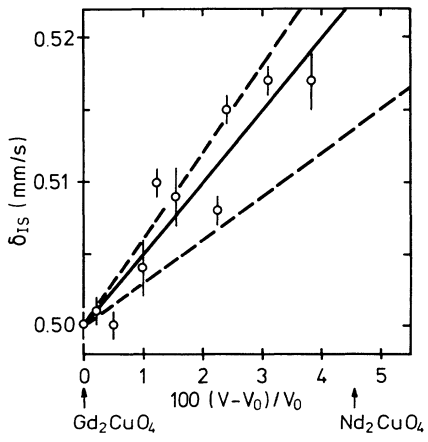

FIG. 12. Variation of the isomer shift δ_{IS} of ^{155}Gd Mössbauer spectra with the unit-cell volume in $(Nd_{1-x}Gd_x)_2CuO_4$. The reference volume V_0 is the unit-cell volume of Gd_2CuO_4, $V_0=180.4$ Å^3. The solid line results from a least-squares fit of a straight line to the data. Dashed lines indicate the extreme limits of volume-dependent shifts expected on the basis of pressure experiments for ^{151}Eu and ^{153}Eu (Ref. 30).

For rare earths whose $4f$ ground state has nonzero orbital angular momentum, such as Nd^{3+} and Pr^{3+}, for example, properties connected with $4f$ electrons are strongly influenced by crystal fields due to nonspherical charge distributions of valence electrons and of ionic and electronic charges in the lattice. Derivations of crystal-field parameters from the $4f$-level splitting observed in Nd_2CuO_4 and in Pr_2CuO_4 by inelastic neutron scattering have led to contradictory results.[13,14,31,32] Thus, supplementary information about crystal fields is of some interest. The lowest-order term in the crystal-field Hamiltonian, the interaction between the $4f$ quadrupole moment $Q_{4f}=\alpha_j\langle r^2\rangle_{4f}$ and the electric-field gradient A_2^0 is related to the quadrupole-interaction term in the nuclear hyperfine Hamiltonian.

If the field due to charges in the lattice is dominant, A_2^0 is proportional to V_{zz}:[33]

$$A_2^0=-\frac{1}{4}V_{zz}\frac{(1-\sigma_2)}{(1-\gamma_\infty)}\ , \tag{9}$$

where σ_2 and γ_∞ are the appropriate Sternheimer (anti)shielding factors describing the modification of A_2^0 and of V_{zz}, respectively, due to the response of closed electronic shells to the field of the external charge distribution. This relation must be considered with caution in the case of compounds in which contributions of valence electrons to V_{zz} and to A_2^0 are important. This is probably true for the cuprates studied as extensive calculations of field gradients in $YBa_2Cu_3O_{7-\delta}$ and in $YBa_2Cu_4O_8$ have shown.[34] However, although similar reservations apply to metallic compounds,[35] estimates of A_2^0 on the basis of experimental V_{zz} values for ^{155}Gd in metallic compounds with help of Eq. (9) have led to agreement of the *sign* of A_2^0 with results deduced from other measurements in nearly all cases.[36] Generally, estimates of the *value* of A_2^0 are less satisfactory.

In Table I we have compiled results for $B_2^0=Q_{4f}A_2^0$ deduced from neutron-scattering data for Pr^{3+} and for Nd^{3+} in T'-structure cuprates.[13,14,31,32] The disagreement between results reported by different groups does not only concern the values, but the sign as well. As both Pr^{3+} and Nd^{3+} have a negative quadrupole moment, the

TABLE I. Results for the crystal-field parameter B_2^0 at rare-earth sites in T'-structure compounds R_2CuO_4, deduced from the field gradient V_{zz} at ^{155}Gd nuclei in Nd-rich compounds $(Nd_{1-x}Gd_x)_2CuO_4$ in the present work, from inelastic neutron scattering in the references indicated.

Reference	B_2^0 (Nd) (meV)	B_2^0 (Pr) (meV)
Present work	0.09	0.3
13	0.90±0.02	
14	−0.20±0.012	
31	−0.21±0.01	
32		0.17±0.08

same sign of B_2^0 is expected for both ions in isostructural compounds.

From the result $V_{zz}=+3.5\times10^{21}$ V m^{-2} determined for ^{155}Gd in Nd-rich compounds [Fig. 6(b)], we obtain $A_2^0=-13$ meV a_B^{-2} ($a_B=5.29\times10^{-11}$ m is the first Bohr radius), using the calculated value[37] of the ratio $(1-\gamma_\infty)/(1-\sigma_2)=200$. With tabulated data for α_j and $\langle r^2\rangle_{4f}$,[38] we derive the values of B_2^0 for Nd^{3+} and for Pr^{3+} in T'-structure cuprates given in the first row of Table I.

The positive sign of B_2^0 is in agreement with that derived in Refs. 13 and 32, in disagreement with the sign of Refs. 14 and 31. An additional item of agreement with the results deduced in Ref. 13 is the occurrence of magnetic splitting of the crystal-field levels implied by our interpretation of the low-temperature specific heat of Nd_2CuO_4 as a Schottky anomaly. Furthermore, the negative sign of A_2^0 is in agreement with the sign of the corresponding crystal-field parameter b_2^0 derived from electron spin resonance (ESR) studies of Gd^{3+} in Pr_2CuO_4 and in Eu_2CuO_4.[39]

V. SUMMARY AND CONCLUSIONS

Our investigations of T'-structure compounds $(Nd_{1-x}Gd_x)_2CuO_4$ by several complementary experimental techniques have led to results that provide new insight into details of structural aspects, of exchange interactions involving rare-earth moments, and of the local electronic structure at Gd sites in the system studied.

In Gd_2CuO_4 and in Gd-rich compounds $(Nd_{1-x}Gd_x)_2CuO_4$ with $x>x_{cr}^s=0.625$, O(1) atoms in the CuO_2 planes are displaced from the symmetrical positions between Cu atoms. Thus, the local symmetry at the rare-earth sites is orthorhombic. Another consequence of these displacements is the occurrence of an antisymmetric exchange interaction involving in-plane components of the Cu moments, leading to a weakly ferromagnetic canting of the Cu moments.

The distortions appear abruptly at $x_{cr}^s=0.625$, accompanied by a discontinuity in the concentration dependence of the lattice parameters a and c. For smaller Gd concentrations, the tetragonal T' structure is undistorted.

In Gd-rich compounds, rare-earth moments order spontaneously below a critical temperature $T_N^R(x)$. The order is antiferromagnetic. The angle $\theta=45°$ between the direction of Gd moments and the crystallographic c axis points to the possibility of a noncollinear moment arrangement.

Upon replacement of Gd by Nd, $T_N^R(x)$ decreases more rapidly with decreasing x than expected for dilution with nonmagnetic atoms.

In Nd-rich compounds, for $x<x_{cr}^m\approx0.4$, ordering of rare-earth moments at low temperatures is induced by dominant exchange interactions between ordered Cu moments and Nd moments. This interaction leads to a magnetic splitting of the crystal-field doublets. The ground-state splitting corresponds to a temperature of 4.5 K. Thermal population of the excited level leads to a Schottky anomaly in the low-temperature specific heat which is only slightly modified by weak Nd-Nd exchange interactions. The Schottky anomaly is hardly affected when Nd is partly replaced by Gd, up to the critical Gd concentration x_{cr}^m.

Isomer shifts deduced from ^{155}Gd Mössbauer spectra indicate a rather low degree of covalent Gd-O bonding. The small variation of the shift with concentration can be explained as an effect of changing atomic volume.

From the electric-field gradient at Gd nuclei, positive values for the crystal-field parameters B_2^0 in Nd_2CuO_4 and in Pr_2CuO_4 are inferred.

Note added in proof. Results of an investigation of crystal-field splittings in Nd_2CuO_4 and in Pr_2CuO_4 by inelastic neutron scattering have just been reported.[41] In the analysis of the experimental data, approximations employed in earlier studies were avoided. Results for the crystal-field parameter B_2^0, converted to the Stevens notation, are $B_2^0=0.09$ meV for Nd and $B_2^0=0.32$ meV for Pr. The remarkable agreement of the values derived from the field gradient V_{zz} at Gd nuclei (Table I, first line) with these results of Ref. 41 is a strong indication for the absence of significant contributions of valence electrons to V_{zz} and to B_2^0 at rare-earth sites.

ACKNOWLEDGMENTS

We thank U. Eckern and P. Fulde for fruitful discussions and for valuable advice concerning several aspects of this work.

APPENDIX

In analyzing quadrupole interactions at Gd nuclei we follow the general convention[33] for labeling the principal axes of the electric-field-gradient (EFG) tensor according to the order

$$|V_{xx}|\le|V_{yy}|\le|V_{zz}| \ . \tag{A1}$$

As furthermore,

$$V_{xx}+V_{yy}+V_{zz}=0 \ , \tag{A2}$$

the principal components are determined by two parameters, V_{zz} and the asymmetry parameter $\eta=(V_{xx}-V_{yy})/V_{zz}$. The convention Eq. (A1) restricts the values η to the range $0\le\eta\le1$. The x and y components of the EFG tensor are given by

$$V_{xx}=-\tfrac{1}{2}(1-\eta)V_{zz}, \quad V_{yy}=-\tfrac{1}{2}(1+\eta)V_{zz} \ . \tag{A3}$$

If the point symmetry group at the site of the probe nucleus contains a symmetry axis S_n with $n>2$ (i.e., $n=3$, 4, or 6), the z axis of the EFG tensor coincides with S_n, and $V_{xx}=V_{yy}=-\frac{1}{2}V_{zz}$, that is, $\eta=0$. This is the situation in Nd-rich compounds with Gd concentrations below $x_{cr}^s=0.625$. At rare-earth sites, there is a fourfold symmetry axis parallel to the crystallographic c axis Hence, the EFG z axis is parallel to the c axis.

In the presence of oxygen displacements in Gd-rich compounds (Fig. 3), the point group at Gd sites is $mm2$. By symmetry arguments, the principal axes of the EFG tensor do coincide with the crystal axes as defined for the tetragonal T' structure. No general rule however, determines the crystal axis, which is singled out as the EFG z

axis according to the convention Eq. (A1).

In case of the continuous evolution of distortions that lower the local symmetry from tetragonal to orthorhombic, a continuous increase of the value η from $\eta=0$ is to be expected. This may proceed until the value $\eta=1$ is reached. For this value of the asymmetry parameter, $V_{xx}=0$ and $V_{yy}=-V_{zz}$. For distortions beyond this, $|V_{yy}|>|V_{zz}|$, and the convention Eq. (A1) enforces an interchange of the y and z axes of the EFG tensor.[40] The continuous variation of the splitting parameter Δ_Q, defined in Eq. (1), with Gd concentration x [Fig. 6(a)] can be taken as an indication that the component V_{cc} parallel to the crystallographic c axis does remain positive for $x>x^s_{cr}$ and that the apparent discontinuous change of the sign of V_{zz} at $x=x^s_{cr}$ actually implies the interchange of y and z axes of the EFG tensor.

However, the discontinuous appearance of distortions at $x=x^s_{cr}$ may be associated with a major change of the charge distribution of valence electrons in the environment of the Gd sites. Thus, we cannot definitely exclude the possibility that the component V_{cc} does change the sign. Then, the continuous variation of both Δ_Q and of the isomer shift could be fortuitous.

The Mössbauer spectra of polycrystalline, texture-free absorbers are fully determined by the direction of the magnetic hyperfine field with respect to the principal axes of the EFG tensor, expressed in terms of polar angles θ_z,Φ_z with the EFG z axis as polar axis. The spectra do not carry any information about the orientation of the principal axes with respect to the crystalline lattice. Hence, for the direction of the Gd moments, which is parallel to the direction of the hyperfine field with respect to the crystal lattice (expressed as θ_c,Φ_c), we have to consider the two possibilities resulting from the two possible orientations of the EFG axes with respect to the crystal axes:

(i) The EFG z axis is parallel to the crystalline c axis. Then $\theta_c=\theta_z$ and $\Phi_c=\Phi_z$ [open circles in Fig. 11(b)].

(ii) The EFG y axis is parallel to the crystalline c axis, the EFG z axis is in the plane perpendicular to the c axis. In this case $\cos\theta_c=\sin\theta_z\sin\Phi_z$, $\tan\Phi_c=\cos\theta_z/(\sin\theta_z\cos\Phi_z)$ [full circles in Fig. 11(b)].

In Gd_2CuO_4, the result for θ_c is nearly the same for both possibilities, $\theta_c\approx 45°$, as shown in Fig. 11(b). Upon replacement of Gd by Nd in the concentration range $0.625\le x<1$, θ_c remains constant near 45° if we assume the z axis to be parallel to the crystallographic c axis. In contrast, if the z axis is perpendicular to the c axis, θ_c increases gradually to a value near 90° as x approaches $x^s_{cr}=0.625$.

[1] A review of experimental results for these compounds was given recently by M. B. Maple, N. Y. Ayoub, J. Beille, T. Bjørnholm, Y. Dalichaouch, E. A. Early, S. Ghamaty, B. W. Lee, J. T. Markert, J. J. Neumeier, G. Nieva, L. M. Paulius, I. K. Schuller, C. L. Seaman, and P. K. Tsai, in *Transport Properties of Superconductors*, edited by R. Nicolsky (World-Scientific, Singapore, 1990), p. 536.

[2] M. Alexander, H. Romberg, N. Nücker, P. Adelmann, J. Fink, J. T. Markert, M. B. Maple, S. Uchida, H. Takagi, Y. Tokura, A. C. W. P. James, and D. W. Murphy, Phys. Rev. B **43**, 333 (1991).

[3] K. C. Hass, Solid State Phys. **42**, 213 (1989).

[4] K. K. Singh, P. Ganguly, and C. N. R. Rao, Mater. Res. Bull. **17**, 493 (1982).

[5] H. Okada, M. Takano, and Y. Takeda, Physica C **166**, 111 (1990).

[6] H. Okada, M. Takano, and Y. Takeda, Phys. Rev. B **42**, 6813 (1990).

[7] S. B. Oseroff, D. Rao, F. Wright, D. C. Vier, S. Schultz, J. D. Thompson, Z. Fisk, S.-W. Cheong, M. F. Hundley, and M. Tovar, Phys. Rev. B **41**, 1934 (1990).

[8] J. D. Thompson, S.-W. Cheong, S. E. Brown, Z. Fisk, S. B. Oseroff, M. Tovar, D. C. Vier, and S. Schultz, Phys. Rev. B **39**, 6660 (1989).

[9] Ph. Galez and G. Collin, J. Phys. (Paris) **51**, 579 (1990); Ph. Galez, P. Schweiss, G. Collin, and R. Bellissent, J. Less-Common. Met. **164&165**, 784 (1990).

[10] T. Moriya, Phys. Rev. **120**, 91 (1960).

[11] S. Ghamaty, B. W. Lee, J. T. Markert, E. A. Early, T. Bjørnholm, C. L. Seaman, and M. B. Maple, Physica C **160**, 217 (1989).

[12] M. F. Hundley, J. D. Thompson, S.-W. Cheong, Z. Fisk, and S. B. Oseroff, Physica C **158**, 102 (1989).

[13] A. T. Boothroyd, S. M. Doyle, D. McK. Paul, D. S. Misra, and R. Osborn, Physica C **165**, 17 (1990).

[14] U. Staub, P. Allenspach, A. Furrer, H. R. Ott, S.-W. Cheong, and Z. Fisk, Solid State Commun. **75**, 431 (1990).

[15] J. W. Lynn, I. W. Sumarlin, S. Skanthakumar, W.-H. Li, R. N. Shelton, J. L. Peng, Z. Fisk, and S.-W. Cheong, Phys. Rev. B **41**, 2569 (1990).

[16] M. Matsuda, K. Yamada, K. Kakurai, H. Kadowaki, T. R. Thurston, Y. Endoh, Y. Hikada, R. J. Birgeneau, M. A. Kastner, P. M. Gehring, A. H. Moudden, and G. Shirane, Phys. Rev. B **42**, 10 098 (1990).

[17] T. E. Mitchell, T. Roy, Z. Fisk, S-W. Cheong, J. D. Thompson, and T. T. Cheng, in *Proceedings of the 47th Annual Meeting of the Electron-Microscopy Society of America*, edited by G. W. Bailey (San Francisco Press, San Francisco, 1989), p. 160.

[18] Y. Tanaka, D. B. Laubacher, R. M. Steffen, E. B. Shera, H. D. Wohlfahrt, and M. V. Hoehn, Phys. Lett. **108B**, 8 (1982).

[19] H. Armon, E. R. Bauminger, and S. Ofer, Phys. Lett. **43B**, 380 (1973).

[20] R. F. Jardim, C. H. Westphal, C. C. Becerra, A. Paduan-Filho, and N. F. Oliveira, Jr., in *Transport Properties of Superconductors*, edited by R. Nicolsky (World-Scientific, Singapore, 1990), p. 183.

[21] L. Pintschovius, N. Pyka, W. Reichardt, A. Yu. Rumiantsev, N. L. Mitrofanov, A. S. Ivanov, G. Collin, and P. Bourges, Physica B **174**, 323 (1991); N. Pyka, N. L. Mitrofanov, P. Bourges, L. Pintschovius, W. Reichardt, A. Yu. Rumiantsev, and A. S. Ivanov, Europhys. Lett. **18**, 711 (1992).

[22] E. T. Heyen, R. Liu, M. Cardona, S. Piñol, R. J. Melville, D. McK. Paul, E. Morán, and M. A. Alario-Franco, Phys. Rev. B **43**, 2857 (1991).

[23] I. Dzyaloshinsky, J. Phys. Chem. Solids **4**, 241 (1958).

[24] T. Thio, T. R. Thurston, N. W. Preyer, P. J. Picone, M. A. Kastner, H. P. Jensen, D. R. Gabbe, C. Y. Chen, R. J. Birgeneau, and A. Aharony, Phys. Rev. B **38**, 905 (1988); M. A. Kastner, R. J. Birgeneau, T. R. Thurston, P. J. Picone, H. P.

Jenssen, D. R. Gabbe, M. Sato, K. Fukuda, S. Shamoto, Y. Endoh, K. Yamada, and G. Shirane, *ibid.* **38**, 6636 (1988).
[25]S. Sugai and Y. Hidaka, Phys. Rev. B **44**, 809 (1991).
[26]R. J. Birgeneau, Y. Endoh, K. Kakurai, Y. Hidaka, T. Murakami, M. A. Kastner, T. R. Thurston, G. Shirane, and K. Yamada, Phys. Rev. B **39**, 2868 (1989); S.-W. Cheong, G. Aeppli, T. E. Mason, H. Mook, S. M. Hayden, P. C. Canfield, Z. Fisk, K. N. Clausen, and J. L. Martinez, Phys. Rev. Lett. **67**, 1791 (1991).
[27]G. Nieva, S. Ghamaty, B. W. Lee, M. B. Maple, and I. K. Schuller, Phys. Rev. B **44**, 6999 (1991).
[28]J. D. Cashion, D. B. Prowse, and A. Vas, J. Phys. C **6**, 2611 (1973).
[29]H. J. Bornemann, G. Czjzek, D. Ewert, C. Meyer, and B. Renker, J. Phys. F **17**, L337 (1987).
[30]E. R. Bauminger, G. M. Kalvius, and I. Nowik, in *Mössbauer Isomer Shifts,* edited by G. K. Shenoy and F. E. Wagner (North-Holland, Amsterdam, 1978), p. 661.
[31]P. A. Alekseev, I. Yu. Arnold, S. E. Voinova, M. G. Zemlyanov, V. N. Lazukov, V. G. Orlov, P. P. Parshin, and I. P. Sadikov, Superconduct. Phys. Chem. Technol. **2**, 184 (1989).
[32]P. Allenspach, S.-W. Cheong, A. Dommann, P. Fischer, Z. Fisk, A. Furrer, H. Ott, and B. Rupp, Z. Phys. B **77**, 185 (1989).
[33]B. D. Dunlap, in *Mössbauer Effect Data Index Covering the 1970 Literature,* edited by J. G. Stevens and V. E. Stevens (Hilger, London, 1972), p. 25.
[34]K. Schwarz, C. Ambrosch-Draxl, and P. Blaha, Phys. Rev. B **42**, 2051 (1990); C. Ambrosch-Draxl, P. Blaha, and K. Schwarz, *ibid.* **44**, 5141 (1991).
[35]R. Coehoorn, K. H. J. Buschow, M. W. Dirken, and R. C. Thiel, Phys. Rev. B **42**, 4645 (1990).
[36]G. Czjzek, V. Oestreich, H. Schmidt, K. Latka, and K. Tomala, J. Magn. Magn. Mater. **79**, 42 (1989); M. Bogé, G. Czjzek, D. Givord, C. Jeandey, H. S. Li, and J. L. Oddou, J. Phys. F **16**, L67 (1986).
[37]R. P. Gupta and S. K. Sen, Phys. Rev. A **7**, 850 (1973).
[38]A. Abragam and B. Bleaney, *Electron Paramagnetic Resonance of Transition Ions* (Clarendon, Oxford, 1970).
[39]D. Rao, M. Tovar, S. B. Oseroff, D. C. Vier, S. Schultz, J. D. Thompson, S.-W. Cheong, and Z. Fisk, Phys. Rev. B **38**, 8920 (1988); C. Rettori, D. Rao, S. Oseroff, R. D. Zysler, M. Tovar, Z. Fisk, S.-W. Cheong, S. Schultz, and D. C. Vier, *ibid.* **44**, 826 (1991).
[40]G. Czjzek, Hyperfine Interact. **14**, 189 (1983).
[41]A. T. Boothroyd, S. M. Doyle, D. McK. Paul, and R. Osborn, Phys. Rev. B **45**, 10 075 (1992).